

Temperature Control of Proton Exchange Membrane Fuel Cell Based on Linear Active Disturbance Rejection Control

Kashangabuye Bahufite Louis

School of Automation, Wuhan University of Technology, Wuhan, China
Email: 2811837898@qq.com

How to cite this paper: Louis, K.B. (2024) Temperature Control of Proton Exchange Membrane Fuel Cell Based on Linear Active Disturbance Rejection Control. *Journal of Power and Energy Engineering*, 12, 1-23. <https://doi.org/10.4236/jpee.2024.125001>

Received: April 23, 2024

Accepted: May 26, 2024

Published: May 29, 2024

Copyright © 2024 by author(s) and Scientific Research Publishing Inc.

This work is licensed under the Creative Commons Attribution International License (CC BY 4.0).

<http://creativecommons.org/licenses/by/4.0/>



Open Access

Abstract

The performance of proton exchange membrane fuel cells is very sensitive to temperature. The electrochemical reaction results directly in temperature variations in the proton exchange membrane fuel cell. Ensuring effective temperature control is crucial to ensure fuel cell reliability and durability. This paper uses active disturbance rejection control in the thermal management system to maintain the operating temperature and the stack inlet and outlet temperature difference at the set value. First, key cooling system modules such as expansion tanks, coolant circulation pumps and radiators based on Simulink were built. Then, physical modeling and simulation of the fuel cell cooling system was carried out. In order to ensure the effectiveness of the control strategy and reduce the parameter tuning workload, an active disturbance rejection control parameter optimization method using an elite genetic algorithm was proposed. When the optimized control strategy responds to input disturbances, the maximum overshoot of the system is only 1.23% and can reach stability again in 30 s, so the fuel cell temperature can be controlled effectively. Simulation results show that the optimized control strategy can effectively control the stack temperature and coolant temperature difference under the influence of stepped charging current without interference or with interference, and has strong robustness and anti-interference capability.

Keywords

Active Disturbance Rejection Control, Elite Genetic Algorithm, Expansion Tanks, Coolant Circulation Pumps, Radiators

1. Introduction

A fuel cell is a device that directly converts chemical energy into electrical ener-

gy. Due to its cleanliness, no pollution and high energy efficiency, it is considered an important direction for new energy applications [1] [2]. Among many fuel cells, proton exchange membrane fuel cells are considered as an energy technology with development potential due to their outstanding characteristics such as low operating temperature, compact structure and high specific energy [3] [4]. In recent years, it has been used in distributed power plants, backup power supplies, electric vehicles and other fields, and has become a research hot spot in the field of new energy [5].

In practical applications, there are dynamic load changes, system disturbances, etc. The resulting temperature changes will affect its output performance and service life. Therefore, effective thermal management is the key to ensuring high performance and long fuel cell life.

The fuel cell cooling system is the key to stabilizing the stack temperature within the optimal range. Excessive temperature will destroy the activity of the catalyst, cause irreversible damage to the fuel cell, and seriously affect the life of the fuel cell; If the temperature is too low, the catalyst activity will be reduced and the operating efficiency will be reduced; When the stack temperature is stabilized at an optimal level, the fuel cell can operate efficiently and the service life can be extended. Therefore, it is of great significance to study the cooling system of water-cooled proton exchange membrane fuel cells [6].

Most scholars use mathematical equations for modeling, but few use Simulink to study the fuel cell cooling system in depth and effectively control the temperature of the model. The physical modeling method based on Simulink has the characteristics of simple model structure, high calculation accuracy and convenient control [7]. Therefore, this paper is based on the Matlab physical modeling platform to establish a fuel cell cooling system simulation model and realize the control of the fuel cell stack temperature.

Niu Zhuo [8] proposed the coolant flow following current control, partially decoupling the air flow and the coolant flow, and then controlling the air flow by designing PID, which can obtain good control effects. However, during the temperature adjustment process, the temperature difference between the coolant entering and exiting the stack cannot be effectively controlled. Excessive temperature difference can easily lead to uneven temperature distribution in the stack, affecting the stable operation of PEMFC.

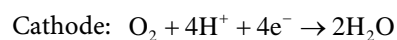
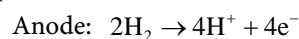
Yang Xiaocai [9] proposed an active disturbance rejection control strategy to control air flow and coolant flow. Taking advantage of the natural decoupling properties of active disturbance rejection control, an active disturbance rejection control system was designed for the flow rates of the two fluids. Through testing, this control strategy has good control effects and can effectively deal with the white noise interference of the galvanometer and thermometer. However, this control system has two active disturbance rejection controllers to control the air flow and coolant flow respectively. Both need to set their own parameters separately, and the parameters influence each other, which makes it difficult to set the parameters, and the system accuracy cannot be guaranteed.

In the traditional control strategy, because the temperature of the fuel cell is difficult to measure, it is assumed that the temperature is equivalent to the coolant outlet temperature. Two PID controllers are designed. One PID controller uses the difference between the coolant outlet temperature and the set value. The value controls the air flow of the radiator, and another PID controller controls the flow of the water pump through the difference between the coolant outlet temperature and the coolant inlet temperature. The traditional PID control requires a total of 6 parameters to be adjusted, and due to the two PID controls. Both controllers use the coolant outlet temperature, so the control signals of the two controllers have strong coupling, which makes it difficult to adjust the parameters and the system accuracy cannot be guaranteed.

This paper makes the following improvements: First, the traditional control strategy that equates the fuel cell temperature to the coolant outlet temperature is abandoned, and the fuel cell temperature is obtained directly through measurement. Nowadays, the internal temperature of a fuel cell can be measured by a variety of methods. The control strategy designed in this work has strong anti-interference performance because it uses active disturbance rejection control. Therefore, the fuel cell temperature does not require too high accuracy. The temperature can be measured using a thermal imager. Secondly, this paper uses the method of flow following current to control the coolant flow, so that the air flow and coolant flow of the radiator are decoupled, and good control effects can be obtained. Third, by designing a first-order linear active disturbance rejection control system to control the air flow of the fan, it can have strong anti-interference and excellent control effects. For setting parameters, an elite genetic intelligent optimization algorithm is proposed to find the optimal parameters. The combination greatly reduces the workload of setting parameters and ensures system control accuracy to a large extent.

2. Proton Exchange Membrane Fuel Cell Model

When the fuel cell is running, the internal hydrogen and oxygen exchange electrons and react to generate water. In this process, hydrogen generates hydrogen ions and electrons in the anode due to the action of the catalyst. The hydrogen ions pass through the proton exchange membrane and reach the cathode. The electrons pass from the anode through the circuit loop and pass through the load, thus doing work on the load, and finally reach the cathode [10]; Oxygen combines with hydrogen ions and electrons in the cathode to form water. The specific chemical reaction is as follows:



During the reaction to generate water, a large amount of heat will be generated. The generated heat will be absorbed by the fuel cell to increase the temperature of the stack, which can improve the catalyst activity and increase the chemical reaction efficiency. However, absorbing too much heat will cause the tem-

perature to be too high, destroy the activity of the catalyst, and cause irreversible damage to the fuel cell. Therefore, a cooling system is required to take away the excess heat so that the fuel cell system can stably operate at a suitable temperature, which can greatly improve the fuel cell system output efficiency and service life.

2.1. Fuel Cell Voltage Model

In order to explore the output characteristics of the fuel cell voltage and simplify the model, obtain the output characteristic curve of the fuel cell and provide an effective basis for subsequent construction of the cooling system model, this section tests the volt-ampere characteristic curve of the stack through relevant experiments. A fuel cell is an extremely complex power generation system, and its output voltage is affected by a variety of external and internal factors. This work mainly focuses on the control research of the cooling system, so the stack voltage output model can be simplified for subsequent research.

The relevant experimental parameter settings are shown in **Table 1**.

Experimental steps: At the beginning of the experiment, set the fuel cell temperature to 80°C; during the experiment, by changing the current, the current increased from 0 to 350 A by 10 A each time, and the output voltage of the system after stabilization at this current was measured, and record each test data [11]. To simplify the output voltage model, this paper uses the U-I data obtained from the experiment of the BP neural network model, with current as the input and voltage as the output. Using MATLAB's own neural network fitting data toolbox for data fitting, the fitting curve of the stack voltage can be obtained, as shown in **Figure 1**.

Table 1. Fuel cell parameters.

Parameter	Parameter value
Number of fuel cells	200
Bipolar plate material	Graphites
Proton exchange membrane reaction area	280 cm ²
Proton exchange membrane thickness	0.0125 cm
Heat dissipation method	Water cooling
Stack temperature	80°C

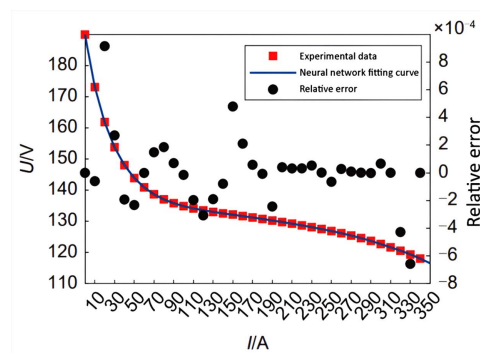


Figure 1. BP neural network fitting characteristic curve.

As can be seen from the figure, the maximum relative error is 0.08%, so the trained BP neural network can represent the stable output voltage of the fuel cell stack under different currents.

2.2. Fuel Cell Temperature Model

When the fuel cell is working, it will generate a large amount of heat and electric energy. The heat generated will help increase the temperature of the stack, thereby improving work efficiency. However, excessive heat will continue to increase the temperature of the stack, thereby destroying the activity of the catalyst and reducing the service life of the fuel cell. Therefore, the excess heat needs to be discharged promptly and accurately to stabilize the stack at a suitable temperature and allow the stack to continue to run efficiently. In order to accurately calculate the heat generated by the fuel cell stack during operation, this paper assumes that all energy in the fuel cell is converted into thermal energy and electrical energy [12]. Based on the first law of thermodynamics, a fuel cell temperature dynamic change model is established [13] (1):

$$C_{st}m_{st}\frac{dT_{st}}{dt} = Q_{gen} - Q_{gas} - Q_{cool} - Q_{atm} \quad (1)$$

In the formula, C_{st} is the specific heat capacity of the fuel cell stack, in $\text{kJ}/(\text{kg}\cdot\text{K})$; m_{st} is the mass of the stack, in kg ; T_{st} is the stack temperature, in K ; Q_{gen} is the fuel heat generation power per unit time, the unit is kJ/s , Q_{gen} can be calculated through the empirical formula [14] (2):

$$Q_{gen} = \frac{(V_0 - V_{fc})I_{st}n}{1000} \quad (2)$$

In the formula, the value of V_0 is related to the state of the reaction product water. This paper assumes that the water generated by the reaction leaves the stack in the form of liquid, then V_0 is 1.482 V. V_{fc} is the output voltage of a single fuel cell, n is the number of fuel cell, is 200.

Q_{gas} is the thermal power taken away by the exhaust gas in the stack, in kJ/s (3). Its value can be expressed by the difference between the heat of the gas leaving and entering the stack [15]:

$$Q_{gas} = Q_{gas,out} - Q_{gas,in} \quad (3)$$

In the formula, $Q_{gas,out}$ and $Q_{gas,in}$ are the heat of the gas entering and exiting the stack respectively, its value is affected by factors such as the flow rate of gas in and out of the stack, gas temperature, air specific heat capacity, and ambient temperature. The mathematical model is relatively complex. According to previous research, 95% of the excess heat of the fuel cell is taken away by the cooling system, while only 5% of the heat is taken away by the exhaust gas in the stack [16] [17] [18]. In order to simplify the model, this paper simplifies its estimation, and its value is (4):

$$Q_{gas} = \frac{5\%Q_{cool}}{95\%} \quad (4)$$

Q_{cool} is the thermal power that the heat flow in the stack penetrates the tube wall and is taken away by the coolant. The unit is kJ/s (5). The expression is:

$$Q_{cool} = \frac{h_1 (T_w - T_{cl,in}) PL}{1000} \quad (5)$$

In the formula, h_1 is the convection heat transfer coefficient, the unit is W/(m²·K); T_w and $T_{cl,in}$ are the tube wall temperature and the stack coolant temperature, respectively, the unit is K; P and L are the cross-sectional circumference of the pipe and the pipe length in the stack, respectively, the unit is m. The convection heat transfer coefficient h_1 is obtained from the definition of Nusselt number [19] (6):

$$Nu = \frac{h_1 D}{k} \quad (6)$$

Nu is the Nusselt number, k is the thermal conductivity, and D is the hydraulic diameter of the pipe. For laminar flow, the Nusselt number is a constant specified based on the pipe geometry and thermal boundary conditions. For turbulent flows, Nu is calculated from the Gnielinski Equation (7)-(9):

$$Nu = \frac{(f/8)(Re_D - 1000)Pr}{1 + 12.7(f/8)^{1/2}(Pr^{2/3} - 1)} \quad (7)$$

$$f = \frac{1}{\left\{ -1.8 \lg \left[\frac{6.9}{Re} + \left(\frac{r}{3.7D} \right)^{1.11} \right] \right\}^2} \quad (8)$$

$$Pr = \frac{C_p \mu}{K} \quad (9)$$

Among them, Re is the maximum Reynolds number when laminar flow occurs, r is the surface roughness of the pipe, C_p is the specific heat capacity of the liquid, and μ is the dynamic viscosity of the liquid.

Q_{atm} is the heat dissipation power of heat exchange between the stack and the environment, in kJ/s (10). Its value is related to the temperature difference and dissipation area. An empirical model can be used [20]:

$$Q_{atm} = \frac{h_2 S (T_{st} - T_{atm})}{1000} \quad (10)$$

In the formula, h_2 is the environmental heat dissipation coefficient, in W/(m²·K); S is the environmental heat dissipation area of the stack, in m²; T_{atm} is the ambient temperature, in K.

This work focuses on the cooling system, so Equation (1) is organized as follows (11):

$$C_{st} m_{st} \frac{dT_{st}}{dt} = Q_{st} - Q_{cool} \quad (11)$$

In the formula, Q_{st} is the sum of the thermal power absorbed by the fuel cell stack and the thermal power taken away by the coolant. The unit is kJ/s and is expressed as (12):

$$Q_{st} = Q_{gen} - Q_{gas} - Q_{atm} \quad (12)$$

2.3. Fuel Cell Thermal Simulation Model

Compared with mathematical modeling, physical modeling is simpler, more accurate and more intuitive. According to Equation (11), the fuel cell stack dynamic temperature simulation model can be built in Simulink, as shown in **Figure 2**.

In **Figure 2**, the controlled heat flow source is an ideal module that can receive the Q_{st} thermal power value through the S signal interface and convert it into a physical signal to participate in the cooling cycle. The thermal mass of the stack is an ideal module, which represents the fuel cell stack. The internal parameters include the total mass of the stack m_{st} and the specific heat capacity C_{st} of the stack.

3. Cooling Circulation System Model

The cooling system mainly consists of coolant, coolant circulation pump, radiator, pipelines and expansion tank. The coolant in the pipeline of the cooling circulation system is powered by a circulating water pump, which takes away the excess heat of the stack and enters the circulation. When passing through the radiator, the air flow is controlled by a fan to discharge part of the heat in the coolant to the environment. The cooling circulation system is stabilized at a suitable temperature to achieve the effect of controlling the stack temperature. The structure of the cooling circulation system is shown in **Figure 3**.

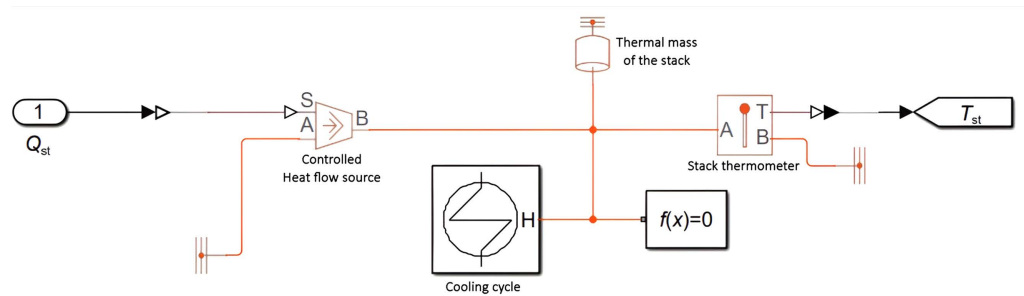


Figure 2. Simulation model of the fuel cell dynamic temperature.

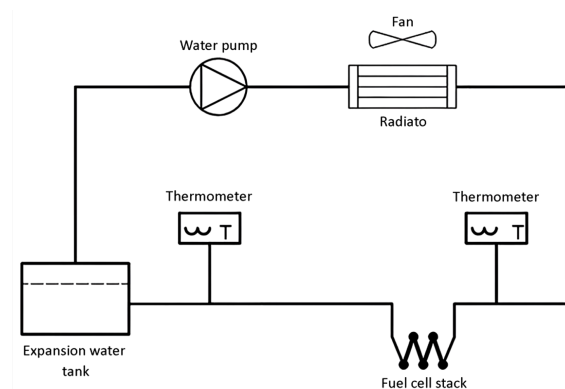


Figure 3. Structure diagram of cooling system.

3.1. Radiator Model

The heat dissipation of the radiator is a function of the heat transfer coefficient, heat dissipation area and temperature difference (13):

$$Q_{loss} = kA(T_w - T_{atm})/1000 \quad (13)$$

In the formula, Q_{loss} is the heat dissipation of the radiator, the unit is kJ/s; k is the heat transfer coefficient of the radiator, its value is related to the material of the radiator and the air flow, the unit is $W/(m^2 \cdot K)$; T_w is the same as T_{atm} are the radiator wall temperature and ambient temperature respectively, in K.

The relationship function between radiator heat transfer coefficient and air flow can be obtained through data fitting. **Table 2** shows the data obtained in reference [21]. Using the fitting tool that comes with MATLAB, you can get the relationship between air flow W_{air} and heat transfer coefficient k (14).

$$k = -4.6W_{air}^2 + 45.17W_{air} + 18.22 \quad (14)$$

3.2. Cooling Circulation System Simulation Model

Based on Equations (5) to (9) and Equations (13) to (14), Simulink was used to build the cooling cycle module in **Figure 2**, which is the cooling cycle system simulation model. As shown in **Figure 4**, the model includes an expansion tank, coolant circulation pump, radiator, etc. The parameter settings of the key model are shown in **Table 3**.

3.3. Verification Model

In order to verify the correctness of the Simulink model of the fuel cell cooling system, the output power of the stack voltage model is maintained at 10 kW. At the same time, the coolant flow and air flow are set according to Yang Xiaocai's master's thesis [9], and the simulation model is stable under different working conditions. The final stack temperature and coolant temperature difference data are compared with the data under the same working conditions in the literature [9]. The results are shown in **Table 4**.

Table 2. Experimental data of heat transfer coefficient [21].

Air flow/(kg/s)	Thermal conductivity coefficient/[$W/(m^2 \cdot K)$]
0	20
0.51	35.63
0.65	42.10
0.78	53.46
0.92	59.47
1.17	66.35
1.22	66.74
1.48	73.46
1.66	79.31
1.76	84.10

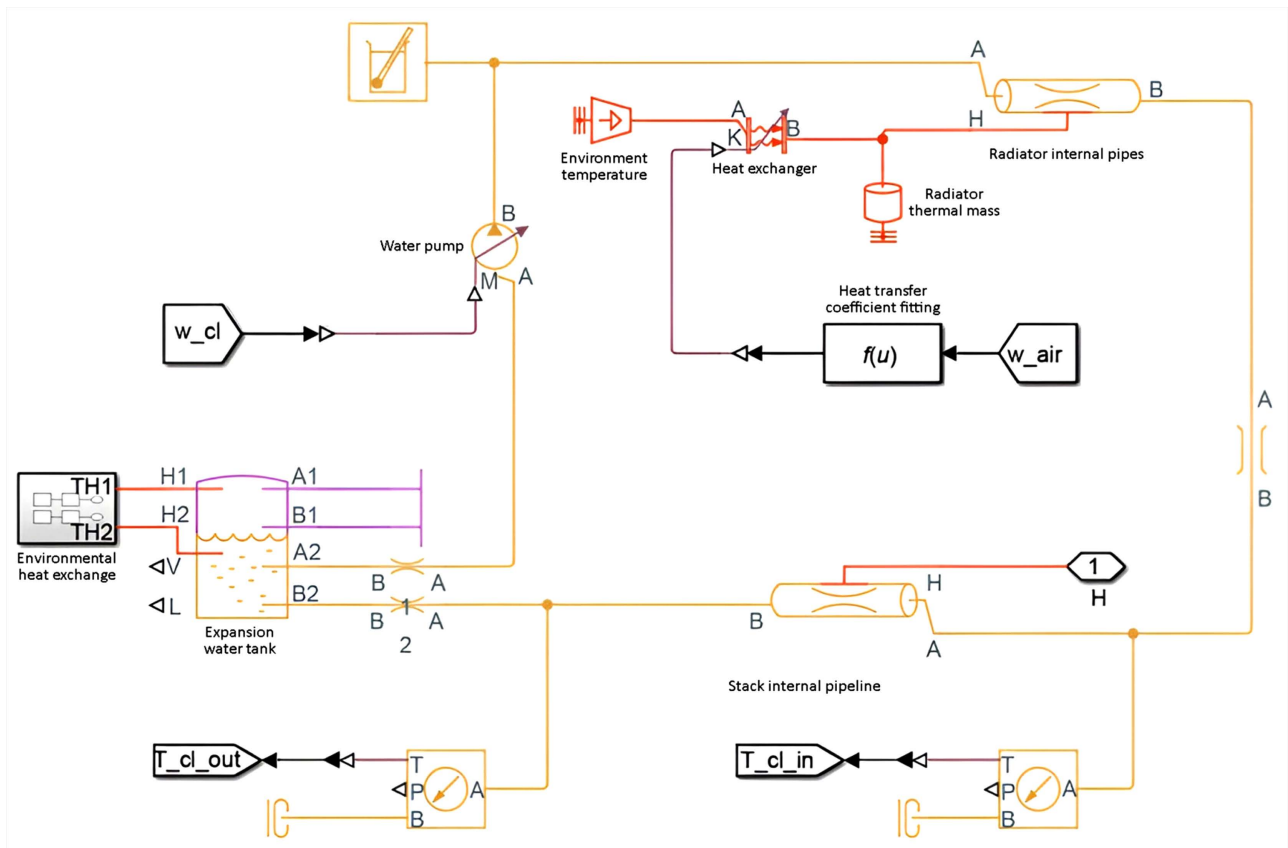

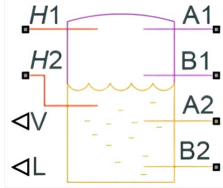
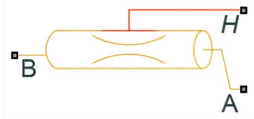


Figure 4. Simulation model of cooling circulation system.

Table 3. Basic parameter table of water pump, radiator and expansion tank model.

Model symbol	Key interface meaning	Parameter name	Parameter value
 <p>Water pump</p>	M: Mass flow control signal kg/s	Pipe cross-sectional area/cm ²	20
 <p>Expansion Water tank</p>	A1, B1: Gas inlet and outlet A2, B2: hot liquid inlet and outlet H1, H2: upper and lower half wall temperatures	Water tank volume/L Water tank cross-sectional area/m ² Entrance and exit cross-sectional area/cm ²	10 0.0625 4.9087
 <p>Stack internal pipeline</p>	H: tube wall temperature	Pipe length/cm Pipe cross-sectional area/cm ² Hydraulic diameter/cm	200.7984 20 1

Continued



Heat exchanger

K: Heat transfer coefficient control signal $W/(m^2 \cdot K)$ Heat exchange area/ m^2

9.3169



Radiator internal pipes

H: tube wall temperature

Pipe length/m

1

Pipe cross-sectional area/ cm^2

9.375

Hydraulic diameter/cm

1



Radiator thermal mass

Mass/kg

3.4521

Specific heat capacity/ $[J/(kg \cdot K)]$

910

Table 4. Temperature data of simulation models and literature [9] under different working conditions.

Output power (KW)	Coolant flow (kg/s)	Air flow (kg/s)	Simulated stack temperature (K)	Simulated coolant temperature difference (K)	Literature stack temperature (K)	Literature coolant temperature difference (K)	Relative error of stack temperature %	Relative error of coolant temperature difference %
10	0.15	0.25	347.4	13.4	345.9	15.68	0.43	-14.54
10	0.25	0.15	359.4	8.84	357.1	8.75	0.64	1.03
10	0.35	0.45	326.61	6.88	325.8	7.53	0.25	-8.63
10	0.45	0.35	330.65	5.11	328.8	5.77	0.56	-11.44

From the comparison of data, it can be seen that the stack temperature obtained by the simulation in this paper is greater than the literature value. This is because the literature value is based on the coolant exit temperature, and the stack temperature is always greater than the coolant exit temperature, which is consistent with the actual situation. The maximum relative error between the simulation results and the literature results is 14.54%, which shows that the established model has strong credibility.

4. Control Strategies

The optimal temperature for proton exchange membrane fuel cell operation is $60^{\circ}C$ to $80^{\circ}C$. The higher the temperature, the higher the battery efficiency; In order to ensure the stable operation of the internal system of the stack, the temperature difference between the coolant entering and exiting the stack cannot exceed $10^{\circ}C$. The smaller the temperature difference, better are the stability.

Control goal: In order to ensure the efficient and safe operation of the fuel cell, the temperature of the fuel cell needs to be controlled and stabilized at 80°C. And the temperature difference between the coolant entering and exiting the stack must be stable within 5°C.

4.1. Design Control Strategy

There is a strong coupling problem in the fuel cell cooling system. The traditional control strategy uses two PID controllers to control the coolant flow and air flow respectively. The control effect is not ideal, and there are certain difficulties in parameter setting of the controller. Based on the above problems, A joint control strategy of cooling water flow following current control and active disturbance rejection control (ADRC) air flow is designed, as shown in **Figure 5**.

4.2. Coolant Flow Follows Current Control Model

There is a strong coupling relationship in the cooling system control. In order to realize the decoupling of the cooling fan and circulating water pump control, current follow-up control is used for the cooling water flow. Based on the current value, calculate the flow rate required to stabilize the coolant temperature difference at 5°C under this current. The coolant flow follows the current, thereby decoupling the fan from the circulation pump.

From formula (11) we can get (15):

$$C_{st}m_{st}\frac{dT_{st}}{dt} = Q_{st} - Q_{cool} = Q_{st} - W_{cl}C_{cl}(T_{cl.out} - T_{cl.in}) \quad (15)$$

In the formula, W_{cl} is the coolant flow rate, unit kg/s; C_{cl} is the coolant specific heat capacity, kJ/(kg·K), $T_{cl.out}$ and $T_{cl.in}$ are the temperatures of coolant entering and exiting the stack respectively, in K; When the stack temperature finally stabilizes, the above formula $\frac{dT_{st}}{dt} = 0$ (16), then

$$Q_{st} = W_{cl}C_{cl}(T_{cl.out} - T_{cl.in}) = Q_{gen} - Q_{gas} - Q_{am} \Rightarrow$$

$$W_{cl} = \frac{0.95(Q_{gen} - Q_{am})}{C_{cl}(T_{cl.out} - T_{cl.in})} \quad (16)$$

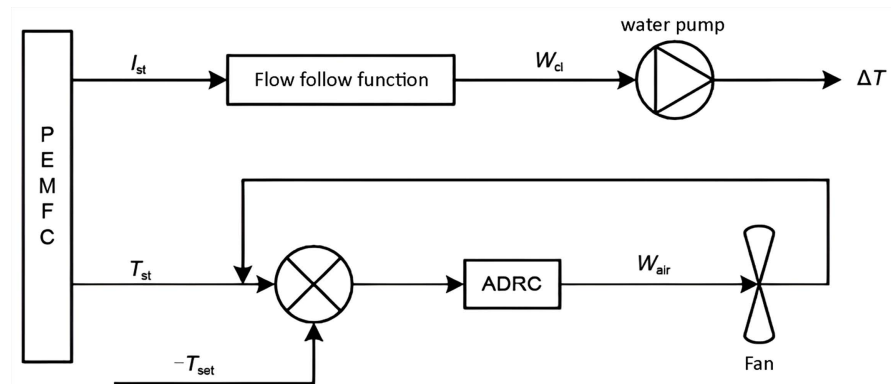


Figure 5. Diagram of the control strategy's structure.

In order to stabilize the temperature difference between the coolant entering and exiting the stack within 5°C, $T_{cl,out} - T_{cl,in} = 5^\circ\text{C}$, and the above formula can be further written as (17):

$$W_{cl} = \frac{0.95 \left[(V_o - V_{fc}) T_{st} n - h_2 S (T_{st} - T_{atm}) \right]}{5 \times 1000 C_{cl}} \tag{17}$$

where V_{fc} is the voltage of a single fuel cell, which can be obtained through the BP neural network fitting model of U-I characteristics.

Based on the above formula, it can be seen that when the stack temperature is stable, the coolant flow rate is only related to the current value. Therefore, the feasibility of the control strategy of the coolant flow rate following the current is theoretically proven.

4.3. Active Disturbance Rejection Control Model

Since the measurement of load current and stack temperature inevitably has certain errors and noise, another controller is needed for precise adjustment and control, and active disturbance rejection control has strong anti-interference ability and strong robustness. The control performance is excellent, so it is very suitable for complex systems such as fuel cell cooling systems with multiple outputs and multiple inputs, nonlinearity, and strong coupling.

4.3.1. Active Disturbance Rejection Control Design

According to Equation (15), the dynamic temperature model of the stack is (18):

$$\begin{aligned} C_{st} m_{st} \frac{dT_{st}}{dt} &= Q_{st} - Q_{cool} = Q_{st} - W_{cl} C_{cl} (T_{cl,out} - T_{cl,in}) \\ &= Q_{st} - kA(T_w - T_{atm}) + w \end{aligned} \tag{18}$$

In the formula, k is the heat transfer coefficient, which is related to the air flow. The linear fitting function relationship expression $k = 36.57u + 20.94$ can be obtained through experimental data; w is the disturbance term.

This system is a first-order system. To facilitate parameter tuning, the controller can use first-order linear active disturbance rejection control. The basic structure is shown in **Figure 6**.

4.3.2. Design of First-Order Linear Extended State Observer

After sorting out formula (18), we can get (19):

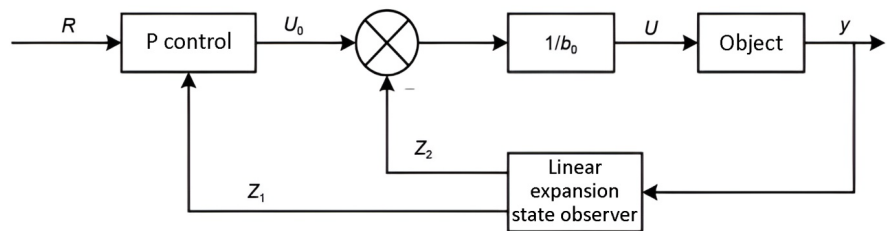


Figure 6. Basic structure diagram of first-order linear active disturbance rejection control.

$$\frac{dy}{dt} = \frac{Q_{st}}{C_{st}m_{st}} - \frac{(36.57u + 20.94)A(T_w - T_{atm})}{C_{st}m_{st}} + w = f + b_o u \quad (19)$$

In the formula, $y = T_{st}$ is the output;

$f = \frac{Q_{st}}{C_{st}m_{st}} - \frac{20.94A(T_w - T_{atm})}{C_{st}m_{st}} + w$ is the total disturbance including external

disturbance and internal disturbance;

$b_o = -\frac{36.57A(T_w - T_{atm})}{C_{st}m_{st}}$ is the input coefficient;

Select the state variables: $x_1 = y$, $x_2 = f$, then $x = [y \ f]^T$ is the expanded state including disturbance, and Equation (19) is transformed into a continuous expanded state space description (20):

$$\begin{cases} \dot{x} = Ax + Bu + Ef \\ y = Cx \end{cases} \quad (20)$$

In the formula, $A = \begin{bmatrix} 0 & 1 \\ 0 & 0 \end{bmatrix}$, $B = \begin{bmatrix} b_o \\ 0 \end{bmatrix}$, $E = \begin{bmatrix} 0 \\ 1 \end{bmatrix}$, $C = [1 \ 0]$.

The corresponding continuous linear extended state observer (LESO) is (21):

$$\begin{cases} \dot{z} = Az + Bu + L(y - \hat{y}) = Az + Bu + L(y - Cz) \\ \hat{y} = Cz \end{cases} \quad (21)$$

In the formula, $z \rightarrow x$, z is the state vector of the observer, L is the error feedback gain of the observer, and $L = [I_1, I_2]^T$. Since \dot{f} is unknown and can be estimated by the observer, \dot{f} is omitted from the above equation. Sorting out the above Equation (22):

$$\dot{z} = (A - LC)z + [B \ L] \times [u \ y]^T \quad (22)$$

Calculating the characteristic roots of $[A - LC]$ gives (23):

$$\lambda(s) = |sl - (A - LC)| = s^2 + I_1s + I_2 \quad (23)$$

After parameterization, the poles of the characteristic equation can be placed at the same position, w_0 (w_0 is the observer bandwidth), that is (24):

$$\lambda(s) = (s + w_0)^2 \quad (24)$$

By combining Equation (24) and Equation (23), we can get $I_1 = 2w_0$, $I_2 = w_0^2$, that is, we can get the state equation of the observer [22] (25):

$$\begin{cases} \dot{z} = \begin{bmatrix} -2w_0 & 1 \\ -2w_0^2 & 0 \end{bmatrix} z + \begin{bmatrix} b_o & 2w_0 \\ 0 & w_0^2 \end{bmatrix} [u \ y]^T \\ \hat{y} = \begin{bmatrix} 1 & 0 \\ 0 & 1 \end{bmatrix} z \end{cases} \quad (25)$$

4.3.3. Linear State Error Feedback Control Law

The classic PID idea can be used to simplify the design of the active disturbance rejection controller. But because the observer can estimate and compensate for external and internal disturbances in real time, moreover, the first-order observ-

er has no differential terms, so the integral terms and differential terms in traditional PID are no longer needed, and the linear state error feedback control law is simplified to the design of P proportion.

For a first-order system, the P controller that can be used for this linear active disturbance rejection control is (26):

$$u_0 = k_p (r - z_1) = y' \tag{26}$$

In the formula, r is a given value, z_1 is the estimated output from the observer, k_p is the amplification factor of the proportion (P), and the Laplace transform of the above formula is obtained (27):

$$k_p [R(s) - Y(s)] = sY(s) \Rightarrow \frac{Y(s)}{R(s)} = \frac{k_p}{s + k_p} \tag{27}$$

Let the root of the characteristic equation of the above formula be, w_0 (w_0 is the bandwidth of the controller), we can get (28):

$$s + k_p = s + w_c \tag{28}$$

Then the P gain of the controller can be obtained as $k_p = w_c$, which simplifies the design of the controller.

4.3.4. Linear Controller Design

The control signal is (29):

$$u = \frac{u_0 - z_2}{b_0} \tag{29}$$

In the formula, z_2 is the disturbance estimate \hat{f} of the observer. Substituting the above formula into formula (19), we can get (30):

$$\frac{dy}{dt} = f + b_0 \frac{u_0 - \hat{f}}{b_0} = u_0 + f - \hat{f} \tag{30}$$

When the observer's disturbance estimate is equal to the true disturbance value, $\frac{dy}{dt} = u_0$, that is, $y = \int u_0 dt$, the system can control the temperature y by controlling u_0 . At this point, the first-order linear active disturbance rejection control design is completed. Based on the above analysis, an active disturbance rejection control air flow simulation model was established, as shown in **Figure 7**.

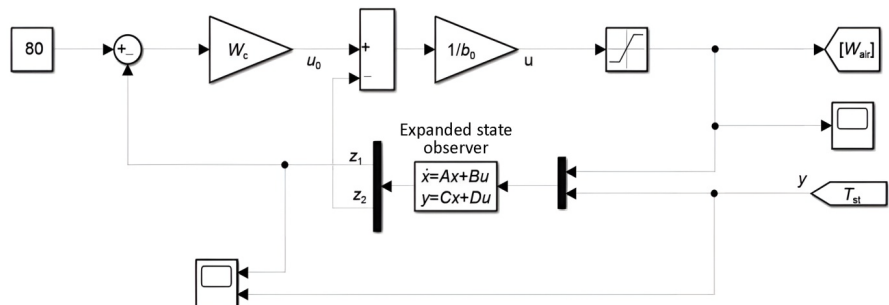


Figure 7. Active disturbance rejection control air flow simulation model.

5. Genetic Algorithm to Tune Active Disturbance Rejection Control Parameters

The active disturbance rejection control has the characteristics of being almost completely independent of the object model, but these parameters need to be adjusted, and the setting of parameters affects the control effect of the system. From the analysis in the previous section, it can be seen that the parameters that need to be tuned for linear active disturbance rejection control are only w_0 , w_c , and b_0 . For most objects, $w_0 \approx (3 \sim 5)w_c$. To simplify the parameter tuning, $w_c = w_0/5$, so that the system only needs to adjust two parameters w_0 and b_0 .

5.1. Genetic Algorithm Design

Genetic Algorithm is an optimization algorithm that solves problems by simulating natural selection and genetic mechanisms. It simulates the process of biological evolution and gradually optimizes solutions through continuous iteration. In genetic algorithms, the fitness function plays a crucial role. It is used to evaluate the fitness of each individual and determine its viability in the evolutionary process. A good fitness function should be able to accurately evaluate the fitness of individuals, so that excellent individuals can be retained while individuals that do not adapt to the environment are eliminated.

In order to avoid switching between decoding and encoding when calculating fitness and reduce the amount of calculation, this paper uses real encoding.

5.1.1. Initializing the Population

The traditional population initialization method will randomly generate multiple feasible solutions, some of which have extremely high fitness values. Due to the existence of these individuals, the quality of population initialization is low and the efficiency of the algorithm is reduced. In order to improve the quality of the initialized population, this paper adopts an elite retention strategy for the initial population, that is, randomly generates multiple populations, calculates the fitness of individuals in each population, and retains individuals with lower fitness values in each population (*i.e.* elite), These individuals are formed into a new population as the initialization population.

5.1.2. Fitness Function

The expression of the objective function is a combination of constraints to be optimized, and is the direct information for the genetic algorithm to search. The constraints of the objective function in this paper mainly consider the integral of the deviation, overshoot time, overshoot amount and adjustment time. In this paper, the smaller the target value, the better the system control effect is (31).

$$\begin{cases} F(i, t) = ts + tp + tr + pos + \int (r - y_i), & y_i < y_{i+1} \\ F(i, t) = ts + tp + tr + pos + \int (r - y_i) + \int (y_i - y_{i+1}), & y_i > y_{i+1} \end{cases} \quad (31)$$

In the formula, ts represents the adjustment time, tp represents the overshoot time, tr represents the rise time, pos represents the overshoot, $\int (r - y_i)$

represents the deviation integral and $\int(y_i - y_{i+1})$ represents the oscillation integral.

5.1.3. Select Operation

This paper combines the roulette selection strategy and the elite selection strategy to design the selection operation, which not only ensures the randomness of the selection operation, but also avoids the loss of the optimal individual, thus improving the convergence speed of the algorithm.

5.1.4. Crossover and Mutation Operations

Crossover uses single-point crossover, select two adjacent individuals, and select a parameter position to perform the crossover operation. Mutation operations increase population diversity and avoid falling into local optimality. **Figure 8** is a flow chart of genetic algorithm tuning linear active disturbance rejection control.

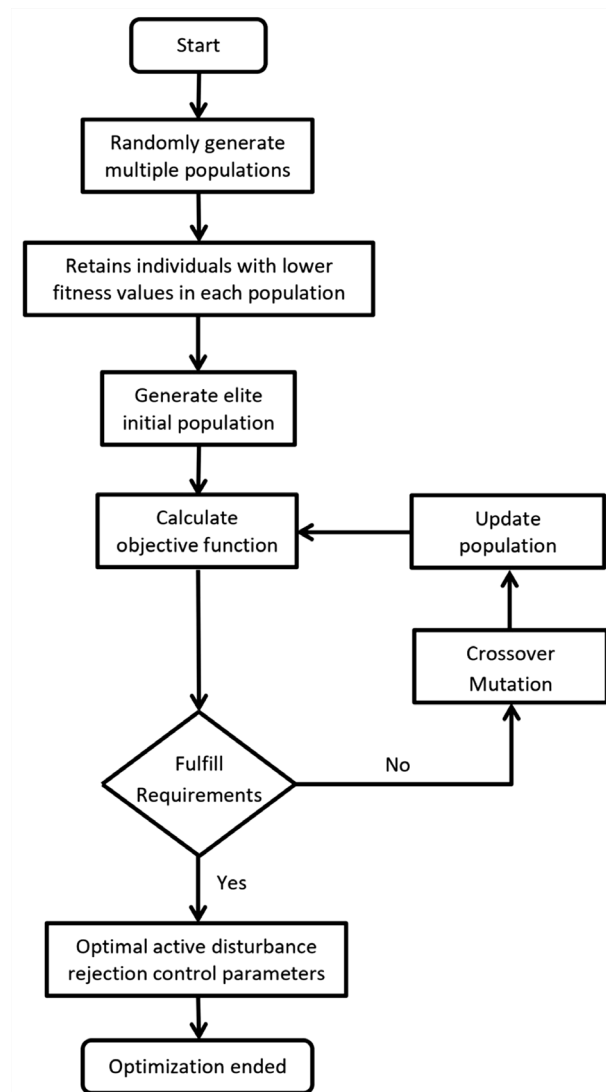


Figure 8. Flow chart of linear active disturbance rejection control parameter optimization using genetic algorithm.

5.2. Genetic Iterative Operations

Each parameter setting: the optimal temperature of the stack is 80°C , the coolant temperature difference is 5°C , the current is set to 100 A; the population size is 20, the crossover probability is 0.8, the mutation probability is 0.2, the number of iterations is 30 generations, and its iteration curve as shown in **Figure 9**.

When iterating 16 times, the fitness value of the optimal individual no longer changes and the optimal parameters of active disturbance rejection controller are obtained.

5.3. Simulation Test

In order to verify the optimization effect of the genetic algorithm on active disturbance rejection controller, the step-changing load current is used as the input, as shown in **Figure 10**; the ambient temperature is set to 25°C . The initial temperatures of the fuel cell and coolant are both set to 25°C ; the control target is to stabilize the stack temperature at 80°C and the coolant temperature difference to be stabilized at 5°C .

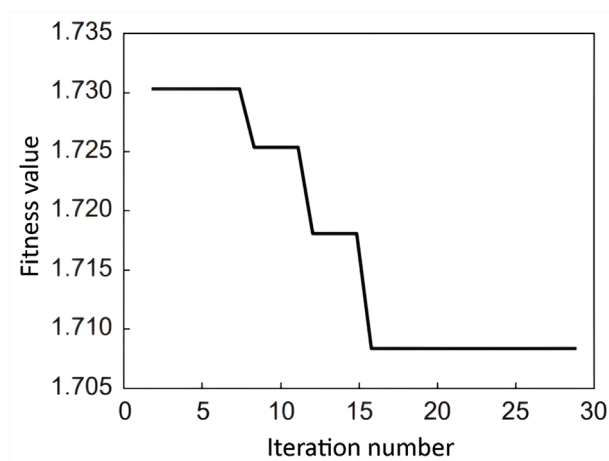


Figure 9. Iteration curve.

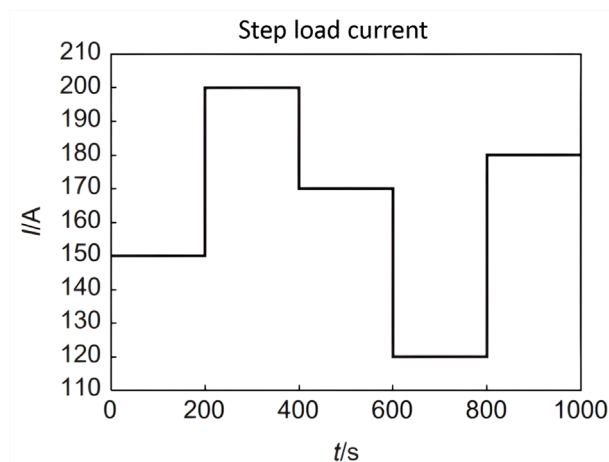


Figure 10. Step load current signal.

Under the influence of step load current, comparing the control effects of conventional and optimized active disturbance rejection controller, the Stack temperature and coolant temperature difference is shown in **Figure 11**, and the air flow adjustment curve is shown in **Figure 12**.

As can be seen from **Figure 11**, the optimized controller has smaller overshoot than the conventional, and the change curve is flatter and has lower volatility, which helps the fuel cell operate more stably under the interference of step load current. As can be seen from **Figure 12**, the optimized fan control performance is significantly improved, the air flow is quickly adjusted to a reasonable value, and the overshoot and fluctuation are smaller, making the fan work more stably. The amount of oscillation is reduced, which is beneficial to improving fan efficiency and extending fan service life.

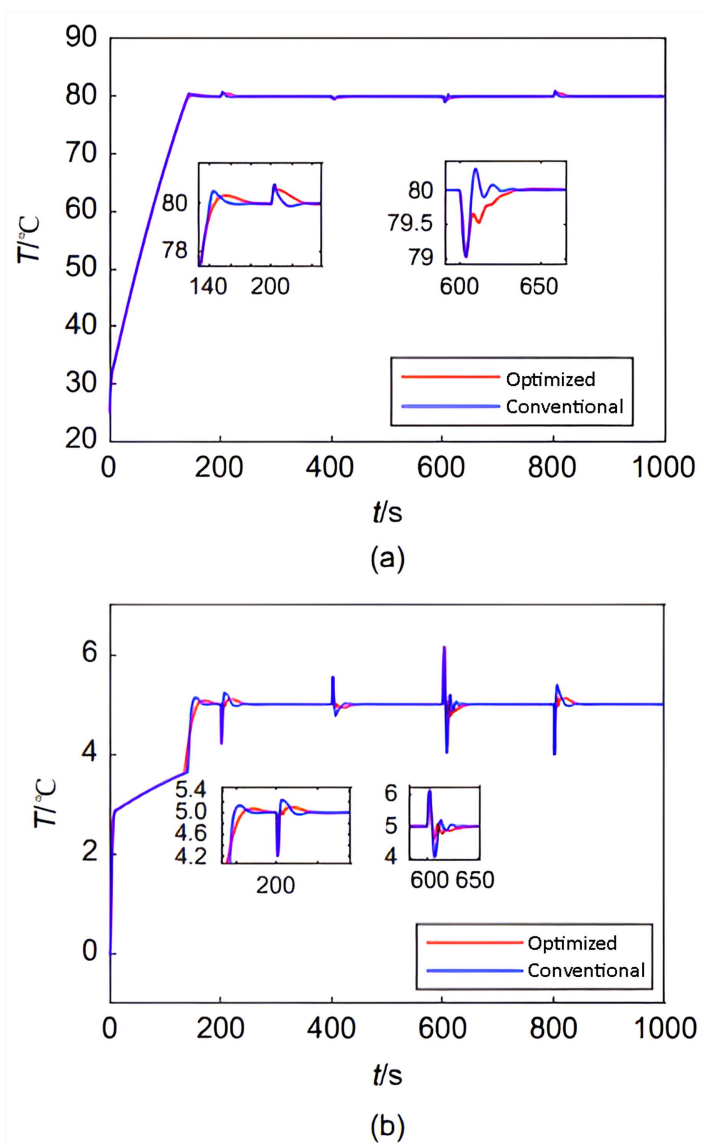


Figure 11. Stack temperature and coolant temperature difference curve under step load current.

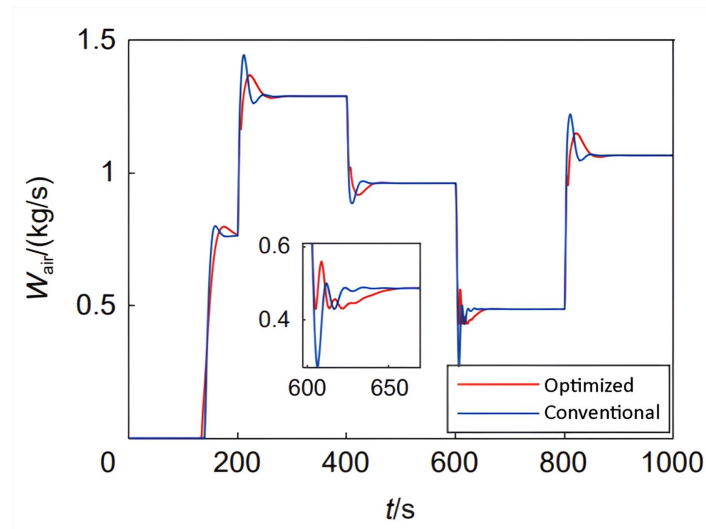


Figure 12. Air flow adjustment curve under step load current.

In order to test the control effect of this control strategy under noise interference, adding noise disturbance to the input load current is shown in **Figure 13**. At the same time, white noise interference is also added to the stack temperature measurement to simulate the real measurement situation. Under the influence of step current and temperature measurements with white noise disturbance, the stack temperature and the temperature difference between coolant entering and exiting the stack are shown in **Figure 14**, and the air flow and coolant flow adjustment curves are shown in **Figure 15**.

Within 130 s, the temperature of the stack rises rapidly due to its own heat generation. The coolant is driven by the water pump to bring heat into the cooling cycle. The coolant heats up rapidly. At this time, in order to avoid excessive heat loss and excessive coolant temperature difference, the air flow rate is input to 0 under active disturbance rejection control. The coolant flow is controlled at a reasonable value by the flow following controller, as shown in **Figure 15**. At 600 s, the load current decreases and the stack temperature decreases due to the decrease in heat production. At this time, the coolant flow rate decreases, causing the coolant temperature difference to temporarily overshoot to 6°C. However, it is still within the safe temperature range and reaches the preset value range again within 30 s, as shown in **Figure 14**. At 800 s, the load current increases by 60 A, the heat generated by the stack also increases, and the coolant flow increases accordingly, causing the coolant temperature difference to briefly drop to 4°C, and the air flow quickly reaches a reasonable value range under active disturbance rejection control, the Stack temperature and coolant temperature difference is again adjusted to the preset value range within 30 s. During this process, the maximum overshoot of the stack temperature is 1.23%. Therefore, when the system is under a step load condition affected by noise disturbance, this control strategy still has good control effect and has strong robustness and anti-interference ability.

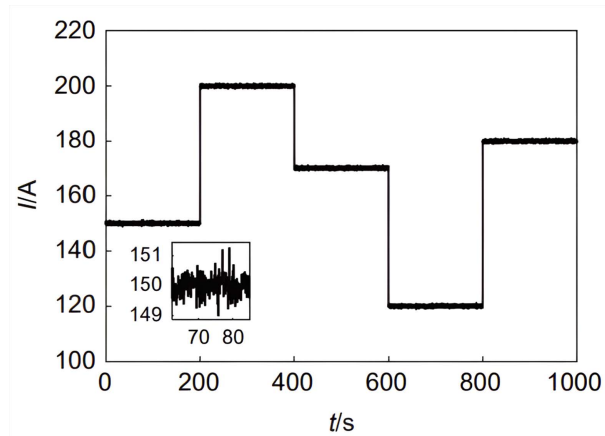


Figure 13. Step load current signal with white noise.

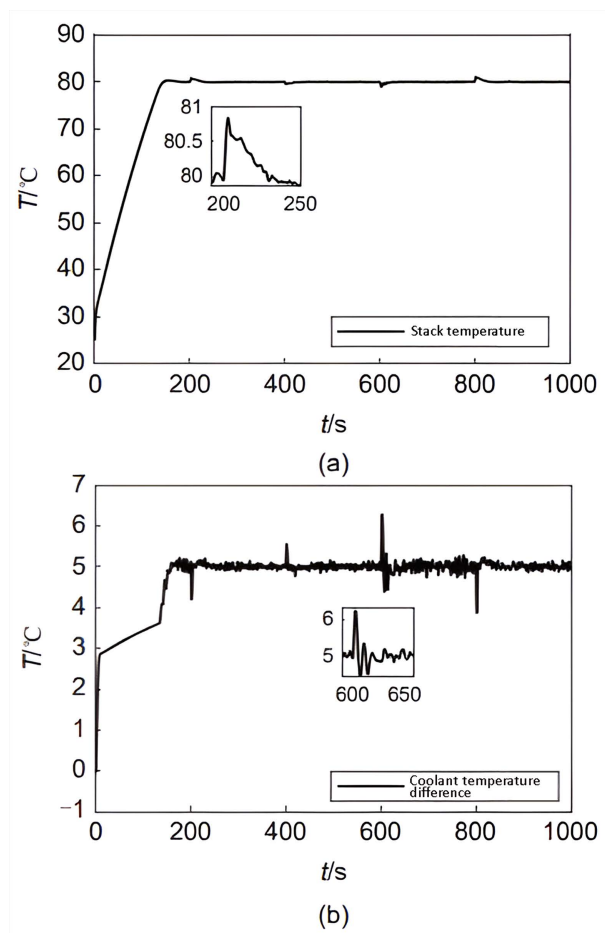


Figure 14. Stack temperature and coolant temperature difference curve under step load current with white noise.

6. Conclusions

To ensure efficient and smooth fuel cell operation and extended service life, it is crucial to stabilize the fuel cell temperature and coolant temperature difference at the optimal temperature.

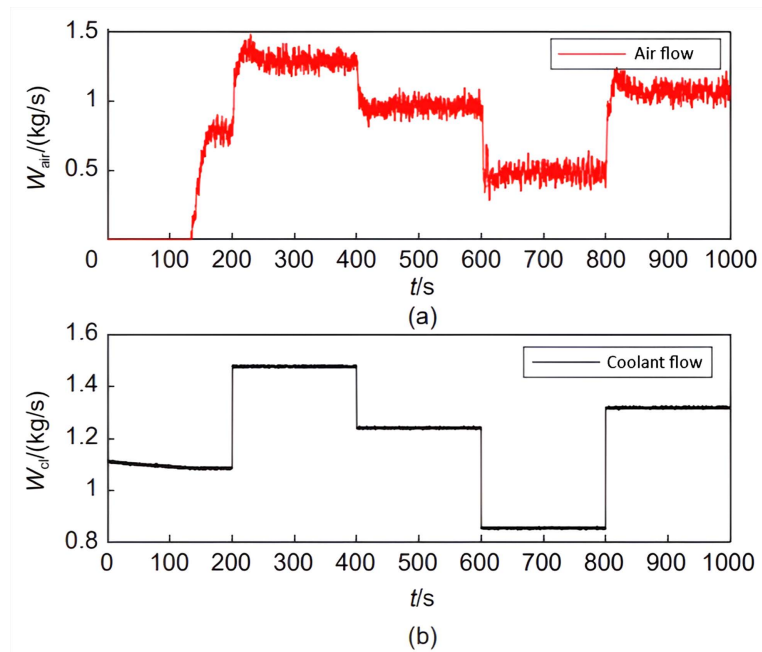


Figure 15. Adjustment curve of air flow and coolant flow under step load current with white noise.

This paper uses experimental data to obtain the U-I characteristic fitting curve of current and voltage, establishes a fuel cell cooling system simulation model through Simulink modeling method, and verifies the reliability of the model; in view of the shortcomings of traditional control strategies, this paper proposes a joint control strategy in which coolant flow follows current control and linear active disturbance rejection control air flow, achieving decoupling of air flow and coolant flow. Due to the challenge of tuning the active disturbance rejection control parameters, the use of elite genetic algorithm optimization is proposed. Effectiveness of the control strategy is ensured by the key parameters. By comparing the control effects of conventional active disturbance rejection controller, it is concluded that the optimized controller has smaller overshoot and smaller volatility, which can effectively improve the working efficiency and service life of the fan. The control effect of this control strategy was tested under a step load current with white noise. The simulation test results showed that under this control strategy, the maximum overshoot of the stack temperature was 1.23%, and the maximum coolant temperature difference was 6°C. When the load current is disturbed, the stack temperature and coolant temperature difference can be adjusted to the preset value range within 30 seconds to ensure that the stack temperature remains stable and evenly distributed, allowing the fuel cell to operate smoothly and efficiently.

Conflicts of Interest

The author declares no conflicts of interest regarding the publication of this paper.

References

- [1] Gu, J., Lu, L. and Ouyang, M. (2007) Thermal Management Subsystem Model and Temperature Control for Fuel Cells. *Journal of Tsinghua University*, **47**, 2036-2039.
- [2] Rahgoshay, S.M., Ranjbar, A.A., Ramiar, A. and Alizadeh, E. (2017) Thermal Investigation of a PEM Fuel Cell with Cooling Flow Field. *Energy*, **134**, 61-73.
<https://doi.org/10.1016/j.energy.2017.05.151>
- [3] Guo, A., Chen, W., Li, Z., Li, Q. and Zhang, L. (2016) Temperature Model and Predictive Control for Fuel Cells in Switcher Locomotive. 2016 35th Chinese Control Conference (CCC), Chengdu, 27-29 July 2016, 4235-4240.
<https://doi.org/10.1109/ChiCC.2016.7554012>
- [4] Gao, F., Blunier, B., Miraoui, A. and El Moudni, A. (2010) A Multiphysics Dynamic 1-D Model of a Proton-Exchange-Membrane Fuel-Cell Stack for Real-Time Simulation. *IEEE Transactions on Industrial Electronics*, **57**, 1853-1864.
<https://doi.org/10.1109/TIE.2009.2021177>
- [5] Cheng, S., Fang, C., Xu, L., Li, J. and Ouyang, M. (2015) Model-Based Temperature Regulation of a PEM Fuel Cell System on a City Bus. *International Journal of Hydrogen Energy*, **40**, 13566-13575. <https://doi.org/10.1016/j.ijhydene.2015.08.042>
- [6] Shan, Y. and Choe, S.-Y. (2005) A High Dynamic PEM Fuel Cell Model with Temperature Effects. *Journal of Power Sources*, **145**, 30-39.
<https://doi.org/10.1016/j.jpowsour.2004.12.033>
- [7] Kiss, T., Lustbader, J. and Leighton, D. (2015) Modeling of an Electric Vehicle Thermal Management System in MATLAB/Simulink. SAE Technical Paper 2015-01-1708, National Renewable Energy Laboratory (NREL), Golden.
<https://doi.org/10.4271/2015-01-1708>
- [8] Niu, Z. (2018) Study on Thermal Management System Control of Watercooled PEMFC. Master's Thesis, Southwest Jiaotong University, Chengdu.
- [9] Yang, X. (2022) Research on Modeling and Control of Water-Cooled PEMFC Cooling System. Master's Thesis, Chongqing University of Technology, Chongqing.
- [10] Huangfu, Y.G., Shi, Q. and Li, Y.R. (2015) Modelling and Simulation System of Proton Exchange Membrane Fuel Cell. *Journal of Northwestern Polytechnical University*, **33**, 682-687.
- [11] Jie, M. (2022) Modeling and Temperature Control Strategy of Air-Cooled Proton Exchange Membrane Fuel Cell Thermal Management System. Master's Thesis, University of Electronic Science and Technology of China, Chengdu.
- [12] Zhao, X., Li, Y., Liu, Z., Li, Q. and Chen, W. (2015) Thermal Management System Modeling of a Water-Cooled Proton Exchange Membrane Fuel Cell. *International Journal of Hydrogen Energy*, **40**, 3048-3056.
<https://doi.org/10.1016/j.ijhydene.2014.12.026>
- [13] Chen, W., Li, Y., Li, Y. and Zhao, X. (2015) Temperature Control Strategy for Water-Cooled Proton Exchange Membrane Fuel Cells. *Journal of Southwest Jiaotong University*, **50**, 393-399.
- [14] Larminie, J. and Dricks, A. (2013) Fuel Cell Systems Explained. 2nd Edition, John Wiley & Sons, Ltd., Hoboken, 1-24.
- [15] Zou, W.-J. and Kim, Y.-B. (2019) Temperature Control for a 5 kW Water-Cooled PEM Fuel Cell System for a Household Application. *IEEE Access*, **7**, 144826-144835.
<https://doi.org/10.1109/ACCESS.2019.2945986>
- [16] Zhou, Y., Chen, J.-L., Zhao, Y. and Xu, S.Z. (2010) Design and Analysis of Cooling System of Fuel Cell Bus. *Shanghai Auto*, No. 1, 19-20+48.

- [17] Xia, M.Z., Xu, S.C. and Li, Y.C. (2005) Design of Fuel Cell Vehicle Cooling System. *East China Electric Power*, No. 4, 1001-9529.
- [18] Guo, S. (2020) Research on Thermal Management System of Proton Exchange Membrane Fuel Cell. Master's Thesis, Hefei University of Technology, Hefei.
- [19] Tiss, F., Chouikh, R. and Guizani, A. (2013) Dynamic Modeling of a PEM Fuel Cell with Temperature Effects. *International Journal of Hydrogen Energy*, **38**, 8532-8541. <https://doi.org/10.1016/j.ijhydene.2012.09.101>
- [20] Hu, P., Cao, G. and Zhu, X. (2011) Temperature Model and Fuzzy Control for the Proton-Exchange-Membrane Fuel Cell. *Control Theory & Applications*, **28**, 1371-1376.
- [21] Wang, X., Sun, J., Chen, N.F. and Yan, L. (2023) Modeling of a Proton Exchange Membrane Fuel Cell Cooling System Based on the Simscape Temperature Control Strategy. *Energy Storage Science and Technology*, **12**, 857-869.
- [22] Zhu, B. (2017) Introduction to Active Disturbance Rejection Control. Beihang University Press, Beijing.